2013

A review of bast fibres and their composites. Part 3: modelling

Summerscales, J

http://hdl.handle.net/10026.1/9926

A Review of Bast Fibres and their Composites. Part 3 – modelling

John Summerscales [a,d], Amandeep Virk [b], and Wayne Hall [c]

(a) Advanced Composites Manufacturing Centre, School of Marine Science and Engineering
Reynolds Building, University of Plymouth, Plymouth, Devon PL4 8AA, United Kingdom.
(b) School of Mechanical and Mining Engineering, University of Queensland,
Brisbane, Queensland 4072, Australia
(c) Griffith School of Engineering, Gold Coast campus, Griffith University, Queensland 4222, Australia

(d) corresponding author. E-mail: jsummerscales@plymouth.ac.uk

Abstract
This paper extends an earlier two-part review of bast fibres and their composites. The paper presents recent statistical models which have been applied to natural fibre reinforcements for composite systems. Recent research suggests that the rules-of mixture should be extended to include the effects of porosity, fibre diameter and yarn twist. A new fibre area correction factor is introduced to correct for the over-estimate of fibre cross-section which occurs when an apparent cross-sectional area is calculated from the "diameter" measured normal to the fibre axis.
Keywords A. Fibres; C. Micro-mechanics; C. Statistical properties/methods

A.   Introduction
A.1   The basics
Statistics is the mathematical science of collecting, analysing, interpreting and presenting data, especially where large quantities of numbers are available. Once the appropriate data set (population) has been identified, it may be possible to analyse the whole data set (population census) or for huge data sets it may be appropriate to consider a sub-set of the population (sample). Descriptive statistics use numerical descriptors including mean and standard deviation for continuous data types (e.g. height or weight), while frequency and percentage are more useful in terms of describing categorical data (e.g. race). Inferential statistics analyse patterns in the population and take account of randomness.

A plot of the normal, or Gaussian, distribution presents a continuous probability distribution with a peak at the mean value, and is often referred to as the bell curve. The arithmetic mean (AM) for a population, μ, is the sum of the values for each item, x_i, divided by the number of items (N) as given by Equation 1a. The arithmetic mean for a sample of that population, $\bar{x}$, is the sum of the values for each item divided by the number of items (n) as given by Equation 1b. The standard deviation (SD) gives an indication of the spread of the data and is calculated using Equation 2a for the entire population or Equation 2b for a sample. The Coefficient of Variation (CoV, Equation 3) measures the scatter of the data points in a data set about their mean. The CoV [1] is useful for the comparison of variations between different variables even if the means of the variables are significantly different.

$$AM\ (population)\ =\ \mu\ =\ \frac{\sum_{i=1}^{N} x_i}{N} \qquad\qquad \text{Equation 1a}$$

$$AM\ (sample)\ =\ \bar{x}\ =\ \frac{\sum_{i=1}^{n} x_i}{n} \qquad\qquad \text{Equation 1b}$$

$$SD\ (population)\ =\ \sigma_{SD}\ =\ \sqrt{\frac{\sum_{i=1}^{N} (x_i^2 - \mu^2)}{N}} \qquad\qquad \text{Equation 2a}$$

$$SD\ (sample)\ =\ s\ =\ \sqrt{\frac{\sum_{i=1}^{n} (x_i^2 - \bar{x}^2)}{n-1}} \qquad\qquad \text{Equation 2b}$$

$$CoV\ (\tau)\ =\ \frac{SD}{AM}\ =\ \frac{\sigma_{SD}}{\bar{x}} \qquad\qquad \text{Equation 3}$$

The whole population has a population variance, σ_{SD}^2. Using the statistical theory for a sample gives a maximum likelihood estimate (MLE) for the mean and Equation 2b eliminates the bias that would arise from using Equation 2a to calculate a variance from the sampled data.

The outer limits of a normal distribution can predict that unlikely values will exist, e.g. negative strengths. Stress is defined as force/area, and as the concept of negative area is alien to the physical world, that

definition in combination with Gaussian statistics could predict compressive failure in tensile tests. Using a log-normal distribution will eliminate this anomaly. Harrop and Summerscales (1989) [2] have reported compressive failures *consequent* upon tensile fracture of armoured cables where the helically-wound reinforcing elements were pultruded Kevlar/epoxy strands.

In data where numbers differ widely, it may be appropriate to use the geometric mean, GeoM, (Equation 4) and geometric standard deviation, GeoSD, (Equation 5) rather than the arithmetic mean and standard deviation.

$$GeoM = \sqrt[N]{\prod_{i=1}^{N} x_i}$$

Equation 4

where Π indicates the product obtained by multiplying the numbers together.

$$GeoSD = \exp\left(\sqrt{\frac{\sum_{i=1}^{N}\left(\ln\frac{x_i}{GeoM}\right)^2}{N}}\right)$$

Equation 5

The relationship between the geometric parameters and the arithmetic parameters is then given by:

$$\bar{x} = \exp\left(\ln(GeoM) + \frac{1}{2}\ln(GeoSD)^2\right)$$

Equation 6 [1]

$$\sigma_{SD} = \exp\left(\ln(GeoM) + \frac{1}{2}\ln(GeoSD)^2\right)\{\exp(\ln(GeoSD)^2) - 1\}^{\frac{1}{2}}$$

Equation 7 [3]

$$CoV = \frac{\sigma_{SD}}{\bar{x}} = \{\exp(\ln(GeoSD)^2) - 1\}^{\frac{1}{2}}$$

Equation 8 [1]

For example, the prediction of the shear modulus (Equation 9) [4] and bulk modulus (Equation 10) [5] of orthotropic ($E_x \neq E_y \neq E_z$ and $\theta=90°$) materials uses the geometric mean.

$$G = \frac{E}{2(1+\nu)} \quad \text{(isotropic)} \qquad G_{12} = \frac{\sqrt{E_1 E_2}}{2(1+\sqrt{\nu_{12}\nu_{21}})} \quad \text{(orthotropic)}$$

Equation 9

$$K = \frac{E}{3(1-2\nu)} \quad \text{(isotropic)} \qquad K = \frac{\sqrt[3]{E_1 E_2 E_3}}{3(1-2\sqrt[3]{\nu_{12}\nu_{23}\nu_{31}})} \quad \text{(orthotropic)}$$

Equation 10

A.2 Weibull statistics

The tensile strengths of both natural and man-made fibres are limited by the presence of critical flaws. In consequence, the fibres exhibit considerable variation in their strengths and strain/elongation-at-break. The probabilistic strength of a material is defined as the loading (stress/strain) which will lead to failure of the material under normal environmental conditions for a given probability (relative frequency of occurrence). The probabilistic strength of a material is obtained by repeating identical experiments to generate a data set of the strengths which is then used to estimate the distribution parameters and allow the probability of failure to be derived from the distribution.

The Weibull distribution is widely used to model diverse life (failure) behaviours and to quantify the spread in the failure indicators of the tested subject (fibre, composite, material, system, *etc*) [6, 7]. Reviews have been published of Weibull statistics for the probabilistic strength of materials [8], for their use in relation to filament strengths [9], for fracture [10] and for the strength [11] of fibrous composite materials.

The two-parameter Weibull Probability Density Function (PDF) is given by Equation 11 [6, 7]. The PDF assumes different characteristic shapes to model different reliabilities and the failure rates. The PDF is dependent on the values of the Weibull distribution parameters: β is the shape parameter (Weibull modulus), η is the scale parameter (the characteristic failure limit, *e.g.* characteristic fibre strength or fibre failure strain) and σ_{UTS} is measured failure limit:

$$f(\sigma_{UTS}) = \frac{\beta}{\eta}\left(\frac{\sigma_{UTS}}{\eta}\right)^{\beta-1} e^{-\left(\frac{\sigma_{UTS}}{\eta}\right)^\beta}$$

Equation 11

Integration of the PDF yields the two-parameter Weibull Cumulative Distribution Function (CDF):

$$F(\sigma_{UTS}) = 1 - e^{-\left(\frac{\sigma_{UTS}}{\eta}\right)^{\beta}}$$

Equation 12

The mean of a Weibull distribution, μ, is given by Equation 13 [7]:

$$\mu = \eta \cdot \Gamma\left(\frac{1}{\beta}+1\right)$$

Equation 13

where the gamma function Γ is given in Equation 14:

$$\Gamma(n) = \int_0^\infty e^{-x} x^{n-1} dx$$

Equation 14

The standard deviation of the Weibull distribution is given by Equation 15 [7]:

$$\sigma_{SD} = \eta \cdot \sqrt{\Gamma\left(\frac{2}{\beta}+1\right) - \Gamma\left(\frac{1}{\beta}+1\right)^2}$$

Equation 15

The coefficient of variation, CoV, for a Weibull distribution is calculated by substituting the equations for the mean (Equation 13) and the standard deviation (Equation 15) in Equation 3:

$$CoV = \frac{\sigma_{SD}}{\mu} = \frac{\sqrt{\Gamma\left(\frac{2}{\beta}+1\right) - \Gamma\left(\frac{1}{\beta}+1\right)^2}}{\Gamma\left(\frac{1}{\beta}+1\right)}$$

Equation 16

Reinforcement fibres for composites exhibit high variability in their mechanical properties. In order to quantify the variation, the probabilistic strength or fracture strain is modelled using the Weibull distribution (e.g. for synthetic [12-17] and natural fibres [18-23]). The probabilistic strength or fracture strain data for the reinforcement fibres can then be used to predict the composite strength [11, 24]. The Weibull statistical fracture theory is used to predict the probability of failure for a random stress state when failure statistics are known for a particular stress state (e.g. tension) [8, 9, 25] and hence permits safety assessment of the system.

The probability of a critical flaw increases with fibre length and hence, longer fibres have lower average tensile strengths and fracture strains. This follows from Griffith's crack theory [26]. The strength at one fibre length is often scaled to estimate the strength at a different length. This is the principle of 'weak link scaling'. The theory assumes that the total volume of the part/system can be conceptually divided into many volume elements and each volume has a small probability of failure and the probability of failure of the system is calculated by multiplying the probabilities of survival of each element [16, 25]. Thus, a larger volume will have a lower probability of survival on average. The Weibull distribution has been used to quantify the variation in the strength of composites [27] and of wood [28, 29] due to size effects. The relationship of the strength (or failure strain) to the fibre length can be modelled using the Cumulative Distribution Function with Weak-Link Scaling (CDFWLS) [18, 30-33]:

$$F(\sigma) = 1 - e^{-\frac{l}{l_o}\left(\frac{\sigma_{UTS}}{\eta_w}\right)^{\beta}}$$

Equation 17

where η_w is the scale parameter (characteristic strength) for the Weibull distribution with weak-link scaling, l is the designated fibre length and l_o is the reference length. For simplicity, the reference length is generally normalised to 1.

The Weak-Link Scaling model does not always represent/quantify the experimental observations [13, 17, 30]. Padgett et al [17] proposed linear and power law models to capture the effect of fibre gauge length on tensile strength. The scale parameter was assumed to be a function of fibre gauge length and the modified Weibull distribution functions are Equation 18 (linear model) and Equation 19 (power law) respectively:

$$F(\sigma) = 1 - e^{-(l+\gamma)\left(\frac{\sigma_{UTS}}{\eta_w}\right)^{\beta}}$$

Equation 18

$$F(\sigma) = 1 - e^{-l^{\gamma}\left(\frac{\sigma_{UTS}}{\eta_w}\right)^{\beta}}$$

Equation 19

where l is the fibre gauge length and γ is a fitting parameter. The Weibull distribution parameters for the model were estimated by the maximum likelihood method [17, 34].

The Weibull distribution parameters are normally estimated using the linear regression or the maximum likelihood methods [6, 7, 34]. Most authors [14, 18] use the linear regression method as it is simple. The Weibull distribution parameters are estimated by rearranging Equation 12 to get Equation 20:

$$\ln\left(-\ln\left(1 - F(\sigma_{UTS})\right)\right) = \beta \ln\sigma_{UTS} - \beta \ln\eta \qquad \text{Equation 20}$$

Equation 20 is in the form $y = mx + c$, where $m = \beta$, $c = -\beta \ln\eta$ and $y = \ln(-\ln(1-F(\sigma_{UTS})))$. The Weibull distribution parameters can thus be obtained from a plot of y against the natural-logarithm of the failure limit σ_{UTS}. $F(\sigma_{UTS})$ is then calculated using the Medial Rank (MR) position [7, 18] of the data points given by Equation 21:

$$MR = \frac{i - 0.3}{N + 0.4} \qquad \text{Equation 21}$$

where i is the failure order and N is the total number of samples. The Weibull parameters are estimated from the slope and intercept of the plot using the linear regression method.

The maximum likelihood method estimates the distribution parameters by maximizing the likelihood function based on the given data set [34]. The maximum likelihood method can be used to fit complex statistical models and the error (or confidence) bound can be calculated for the distribution parameters [30].

B.   Natural fibres and their composites

The state-of-the-art in bast fibres and their composites has recently been reviewed by a number of authors [35-52]. However, the majority of papers simply present the methodology and results obtained. In this review we summarise those papers which contribute to advances in modelling of natural fibre reinforcements and their composites.

C.   Fibres and fabrics

Virk et al [53] used confocal scanning laser microscopy and digital image analysis to quantify the cross-sectional area (CSA) of 106 jute fibres. The fibre CSA was modelled using different geometrical shapes (major circle, minor circle, ellipse, super ellipse, convex hull) and the fibre area was estimated for each individual case. The area distribution for each case was determined and for all the assumed shapes (except for the minor circle) it was observed that the area distribution showed a negative skew indicating that the method overestimates the fibre area. The fibre CSA calculated assuming an elliptical cross-section gave a lower variation in the fibre area compared to the circular cross-section. The minimum elliptical area calculated from the two orthogonal projection widths (a and b) gives the area closest to the true fibre area. Any fibre area calculated using a method that over-estimates the fibre area will always underestimate the modulus and strength of the fibre. Thus, using the ellipse will yield an underestimate of modulus or strength and hence will result in a safer mechanical design when the fibres are used as reinforcement in a composite.

Virk et al [54] proposed that there should be a "fibre area correction factor", κ, to account for the non-circular cross-section of the fibre. For the jute fibres in the study, they measured the apparent fibre diameter (i.e. projected width) by microscopy transverse to the fibre axis for 785 fibres and correlated the data to the measured true cross sectional area of the 106 jute fibres referred to above (taken from the same roll of material as the 785 fibres). The geometric means for the apparent fibre area and the measured true fibre area were 2697 μm^2 and 1896 μm^2 respectively thus giving a fibre area correction factor κ of 1.42.

Aslan et al [55] measured cottonised flax fibres to determine the apparent CSA using optical microscopy transverse to the fibre axis (399 fibres) and the true CSA using electron microscopy of polished embedded samples (585 samples). Their reported data gives a fibre area correction factor κ of 1.39 (327 and 236 μm^2 respectively). For the same fibre set, the mean lumen content was 1.6% with >85% of fibres having a lumen content <1%.

Thomason et al [56] measured the CSA of individual fibres using transverse optical microscopy of fibres mounted on cards and optical microscopy of polished embedded cross-sections. Linear fits of data on

plots of *cross-section calculated from apparent diameter* against *true cross-section* had slopes of 2.55 (flax) and 1.99 (sisal) albeit with R^2 of 0.46 and 0.43 respectively. Twelve individual fibres from each plant were measured at ten positions along a 21 mm length of each fibre. The average CSA at the centre or at the ends of the gauge length were greater than the overall respective means and within a range of <15% CSA implying that CSA is independent of position along the fibre.

Cosson et al [57] have developed a procedure using optical images of light transmission through samples of reinforcement to experimentally measure the spatial variation in areal weight of an isotropic chopped strand mat. For samples from a single roll of quasi-unidirectional jute reinforcement, Virk [58] recorded an areal weight of 880 g/m^2 at the outside of the roll while Bradbury [59] reported the areal weight to be 669±60 g/m^2 (CoV = 9%) closer to the centre of the roll.

D: Mechanical properties of fibres

The commercial use of natural fibres as the reinforcement for composites is constrained by a perceived high variability in strength. In an examination of tensile test data from 785 individual tests, Virk et al [60] found that the coefficient of variation (CoV) for failure strain is consistently lower than the CoV for fracture stress (strength). The use of optical microscopy to determine fibre "diameter" and hence cross-sectional area may explain this difference as the strength is normally calculated from an assumed cross-sectional area (CSA). The use of failure strain as the key design criterion was recommended for natural fibre composites in order to improve reliability in the design of natural fibre-reinforced composites.

Zafeiropoulos and Baillie [23] have shown that the linear regression and the maximum likelihood methods give similar distribution parameters in their work on the tensile strength of flax fibres with different surface treatments. Several authors [e.g. 30-33] have reported that the failure strength and failure strain distribution of natural fibres can be described by two-parameter Weibull distributions.

Andersons et al [12] found that the strength distribution of fibres sampled from an E-glass fibre bundle agreed with the two-parameter Weibull distribution at each of the gauge lengths considered (*i.e.* 5, 10, 20, 40 and 80 mm). However, the Weibull distribution shape parameter determined from the average strength *vs.* length data was considerably higher than that obtained at a fixed gauge length. They suggested that for their data, the standard Weibull distribution was not applicable to the fibre batch strength, while a modified Weibull distribution was found to provide good agreement with the strength data. The Weibull parameters derived from fibre bundle tests (FBT) for 80 mm gauge length samples agreed reasonably well with the single fibre test (SFT test) results, while at longer gauge lengths (160 and 320 mm) the FBT yields lower shape parameter values. They attributed their results to the presence of widely spaced random damage in the fibre bundles due to processing and handling. Single fibre fragmentation (SFF) tests revealed that fragmentation proceeds in agreement with the standard Weibull strength distribution, but the distribution parameters for individual fibres possessed a marked scatter. The average Weibull shape parameter from SFF was larger than that derived from SFT at constant gauge length, but near the value obtained from mean strength *vs.* length data. The agreement of SFT and FBT test results with a standard Weibull distribution at a single gauge length may be misleading, so they recommend that tests at several gauge lengths should be performed to reveal the length dependence of fibre strength. The Weibull distribution shape parameter determined from the average strength vs. length data was higher than that for a fixed gauge length. A modified Weibull distribution (Equation 22) provided good agreement with the strength data for the glass fibres considered.

$$F(\sigma) = 1 - e^{-\left(\frac{l}{l_o}\right)^{\gamma}\left(\frac{\sigma}{\beta_\sigma}\right)^{\alpha}}$$
<div align="right">Equation 22</div>

where independent exponents characterise the mismatch of the fibre strength scatter at a fixed gauge length (α) and the average strength dependence on the fibre length (governed by γ/α). The modified Weibull distribution shows the weakest link scaling only when γ=1.

Andersons et al [18] conducted SFT tests on elementary flax fibres at several gauge lengths to obtain strength and failure strain distributions. Both parameters were found to follow the modified Weibull distribution (Equation 22). Both the strength scatter at a fixed gauge length and the dependence of mean strength on fibre length should be characterised. SFF tests revealed that the fibre fragmentation process again proceeded in agreement with the two-parameter Weibull distribution of failure strain, but with a marked scatter in the distribution parameters for individual fibres.

Virk et al [61] conducted one hundred tensile tests at each of five distinct fibre lengths (6, 10, 20, 30 and 50 mm) on a single batch of jute fibres from South Asia. For the jute fibres tested, the Young's modulus was found to be ~30 GPa while the ultimate strength and fracture strain are reduced from 558 to 336 MPa and from 1.79 to 1.11% respectively as the length increases from 6 to 50 mm. Weibull parameters for the jute fibres were estimated for each fibre length using a maximum likelihood estimate (MLE, referred to as point estimates). Based on the point estimates, two empirical models (a linear and a natural logarithmic interpolation model (NLIM)) were developed to characterise the ultimate strength and fracture strain across the entire range of the fibre lengths tested (i.e. 6–50 mm). The logarithmic interpolation model for ultimate strength and fracture strain was found to produce a better fit to the point estimates (i.e. at the five distinct fibre lengths) than the linear model. Both models produce a better estimation for ultimate strength than for fracture strain.

The same authors [62] tested jute technical fibres in tension at ten different gauge lengths between 6 mm and 300 mm with 50 or 100 tests at long or short gauge lengths respectively to determine the Young's modulus, strain to failure and ultimate tensile strengths for each individual fibre. Weibull distribution parameters calculated using the maximum likelihood parameter estimation method were used to quantify the variation. Single parameter (standard) and Multiple Data Set (MDS) weak-link scaling predictions were assessed using Anderson–Darling Goodness of Fit Numbers (GOFN). The authors recommend the use of MDS weak-link scaling for this problem. The weak-link scaling should be performed with at least two points. It is preferable to use three points with the fibre length at two extreme points and a third point near the mean fibre length.

In reference [63], they extended the previously reported NLIM analysis (for fibres up to 50 mm long) to include fibres with lengths up to 300 mm. The NLIM produces a significant improvement in predicted properties over the MDS model. The use of Anderson–Darling GOFN confirms this finding and reveals a reduction factor (MDS model GOFN/logarithmic model GOFN) for this measurement of 2.74 for strength and 2.23 for strain.

Andersons et al [64] proposed that Equation 22 could model the strength distribution of elementary flax fibres when the strength-length scaling exponent, γ_σ, used to characterise the interfibre variability is related to the scatter in kink band spacings, s, between the fibres. If m is the shape parameter of the spacing distribution, then γ_σ is given by Equation 23. In the limiting case of almost identical intervals between kink bands, $m \gg 1$, γ_σ tends to unity and the equation reverts to the classical Weibull distribution for fibre strength. The approximate analytical distribution function has been verified against experimental data.

$$\gamma_\sigma = \frac{m}{\sqrt{m^2 + 1}}$$

Equation 23

Bast fibres differ from man-made fibres in that they are subject to damage due to exposure to the weather, harvesting and subsequent fibre extraction processes. The flexural loads encountered result in compression and shear failures. These *defects* are variously referred to as dislocations, kink bands, nodes or slip planes [65], although the terms are often used interchangably. Dai and Fan [66] examined 1000 hemp fibres, and present photomicrographs of the four types of defect although their rationale for the separation of each form is not clear. Thygesen [67] has proposed that there is a correlation between the effective fibre bundle strength (σ_b) and the number of processing steps which fits an exponential curve:

$$\sigma_b = \sigma_{b,0} (1 - r)^N$$

Equation 24

where $\sigma_{b,0}$ is the effective bundle strength of unprocessed fibres and r is a constant reduction factor per processing step (found to be 0.27 for the flax and hemp fibres studied).

Andersons et al [68] have derived a strength distribution function to explicitly account for the presence of such defects. If the probability that a length of fibre contains a defect is p and that the probability that the fibre is defect-free is 1-p, then the strength distribution for the system will depend on the maximum number of defects in the fibre, n. If the maximum number of defects in a fibre is a power function of its length, n(l), then the fibre strength distribution function will be:

$$F(\sigma) = 1 - \left(1 - p \left(1 - exp \left(- \left(\frac{\sigma}{b} \right)^a \right) \right) \right)^{n(l)}$$

Equation 25

Experimental confirmation of this relationship between the distribution of defects and the fibre strength distribution requires further research.

E. Microstructures of fibres and composites

Guild and Summerscales [69] and Summerscales [70] have reviewed the use of microscopy and image analysis for the characterisation of fibre-reinforced composite systems. Summerscales et al [71] used image analysis to quantify microstructural features of woven fabric composites. Even when no difference could be discerned by eye, the microstructures could be distinguished using Voronoi tessellation and Fractal Dimension and the data correlated to laminate permeability and mechanical properties. These parameters (and possibly lacunarity) appear to show good promise for the development of process-property-structure relationships, although they have not yet been used in the context of natural fibre composites. A major constraint is the difficulty (especially in optical microscopy) of obtaining good contrast between the fibre and matrix phases without altering the structures under observation.

F. Mechanical properties of composites

The Young's modulus of a solid decreases with increasing porosity. This was first analysed theoretically by Mackenzie [72] for the case of a solid containing spherical holes. Wachtman [73] has summarised the nineteen different equations proposed by various authors for the porosity dependence of elastic moduli in isotropic materials. Davidge [74] has suggested that many of these are in the form:

$$E_p = E_d(1 - f_1 V_p + f_2 V_p^2)$$

Equation 26

where E_d is the modulus of the full density material, E_p is the modulus of the porous material, f_1 and f_2 are constants and V_p is the volume fraction of pores.

Madsen and Lilholt [75] presented a modified rule of mixtures for natural fibre composites to include a simplified term for the influence of porosity on both the axial and transverse composite properties:

$$E_p = E_d(1 - V_p)^2$$

Equation 27

Toftegaard and Lilholt [76] and Madsen et al [77] extended the model to include a variable exponent:

$$E_c = (\eta_l \eta_o V_f E_f + V_m E_m)(1 - V_p)^{n_E}$$

Equation 28

$$\sigma_c = (\eta_l \eta_o V_f \sigma_f + V_m \sigma_m \cdot)(1 - V_p)^{n_\sigma}$$

Equation 29

where E_x is the elastic modulus of the component, σ_x is the strength, V_x is the volume fraction of the component (assuming $V_f + V_m + V_p = 1$, i.e. voids but no other inclusions), the subscripts (x) for components are c for composite, f for fibres, m for matrix and p for porosity, η_l is the fibre length distribution factor, η_o is the fibre orientation distribution factor and n_E and n_σ are the respective *porosity efficiency exponent* (PEE) quantifying the effect of porosity which causes stress concentrations in the composites. When the PEE = 0, the porosity in the composite has no effect beyond lowering the load bearing volume. The model was validated with experimental data for volumetric composition and stiffness for several (plant) fibre composites.

The fibre orientation distribution factor can be predicted using the Krenchel equation [78]:

$$\eta_o = \sum_{i=1}^{180^{\cdot}} (V_{f_i} \cos^4 \theta_i)$$

Equation 30

where θ_i is the angle of the fibres to the reference direction. If deriving an off-axis angle for quasi-unidirectional (i.e. sliver with some waviness) it is important to use the mathematical modulus of the respective angles before reporting the degree of misalignment as an average of the true values will return a value closer to zero.

The elastic modulus of bast fibres reduces with increasing fibre diameter. The data for fibres assuming a linear ($E_f = E_{f0} - md$) decline in modulus with increasing fibre diameter for various natural fibres is given in Table 1.

Table 1: Data for linear reduction of modulus with increasing fibre diameter

Fibre	E_{f0} (GPa)	m (GPa/μm)	$(E_{f0} - E_f)/E_{f0}$ (%)	Source	Reference
Flax	86.0	1.4	1.6	Lamy and Baley	79
Jute	45.3	0.3	0.6	Virk et al	61
Nettle	150.6	3.3	2.2	Bodros and Baley	20

Summerscales et al [45, 80] proposed that a fibre diameter distribution factor, η_d, should be included in the rule-of-mixtures as in Equation 31 to reflect this dependence:

$$E_c = \eta_d \eta_l \eta_o V_f E_f + V_m E_m$$

Equation 31

Virk et al [54] introduced the fibre area correction factor, κ (see Section C), into the rule of mixtures to address the discrepancy between the true cross-sectional area of the non-circular fibre and the apparent cross-sectional area calculated by measurement of the apparent diameter. Their proposed full rules-of-mixture equations for natural fibre composites are:

$$E_c = \kappa \eta_d \eta_l \eta_o V_f E_f + V_m E_m$$

Equation 32

while the Kelly-Tyson equation for the strength of unidirectional composites becomes:

$$\sigma_c' = \kappa \sigma_f' V_f + \sigma_m \cdot V_m$$

Equation 33

where σ' is the ultimate strength and σ_{m*} is the stress in the matrix at the failure strain of the fibre. Figure 1 [54, 81-87] plots elastic modulus data derived from experiments reported in the scientific literature using the standard form of rule of mixtures with $\eta_l=1$ and η_o given appropriate values (blue) and Equation 32 (red). In the majority of cases, the latter equation gives a closer estimate of the experimental data.

Using $\lambda = (1-V_p)$, the inclusion of the effect of matrix porosity in Equation 32 gives:

$$E_c = (\kappa \eta_d \eta_l \eta_o V_f E_f + V_m E_m)\lambda^n$$

Equation 34

or if the porosity is present only in the matrix, this may become:

$$E_c = \kappa \eta_d \eta_l \eta_o V_f E_f + V_m E_m \lambda^n$$

Equation 35

The models of Rao and Farris [88] and Naik and Madhavan [89] for the tensile modulus of impregnated yarn (twisted filaments) account for anisotropy, fibre migration and microbuckling. However, these models are complex and require input data which is not easy to obtain (e.g. all nine elastic constants for an orthotropic material). Baets *et al* [90, 91] have found good agreement between the above predictive models and their experimental data from unidirectional flax yarn/epoxy composites.

Madsen *et al* [92] derived an expression for the mean twist angle, θ_{mean}, in a yarn by integrating the weighted contribution from the core ($x=0$) to the yarn surface ($x=r$) and found that this parameter is a function of the yarn surface twist angle, α:

$$\theta_{mean} = \int_{x=0}^{x=r} \frac{2\pi x}{\pi r^2} \tan^{-1}\left(\frac{2\pi x}{L}\right) dx = \alpha + \frac{\alpha}{\tan^2 \alpha} - \frac{1}{\tan \alpha}$$

Equation 36

Shah *et al* [93] replaced the fibre orientation distribution factor, η_o, in Equation 29 with $\cos^2 q$ (where $q = \alpha$ or 2α) to model the strength of twisted yarn NFRP assuming zero porosity:

$$\sigma_c = \eta_l \cos^2 q \, V_f \sigma_f + V_m \sigma_m$$

Equation 37

Equation 37 is similar in form to that used to model the effect of microfibril angle on the elastic modulus of single plant fibres by McLaughlin and Tait [94]. The $\cos^2(2\alpha)$ model was found to be a near-perfect fit for experimental data from Goutianos and Peijs [95] for aligned flax yarn composites with either 609 tex long fibres or 1000 tex short fibres at seven different twist levels.

The recently proposed models above have only been validated for limited data sets. It would be appropriate for other researchers to confirm or refute the applicability of these models. The development of these approaches should help to bring natural fibre composites to wider application.

G   Conclusions

This paper has reviewed a number of models proposed for bast fibres and their composites. A major constraint on the adoption of these fibres as reinforcements is the reported variability of the mechanical properties. The variation is greater for modulus and strength than for strain to failure due to an assumption of circular fibre cross-sectional area (CSA) and the use of an "apparent diameter" in calculation of the stressed area. A fibre area correction factor (FACF) has been proposed for correction of the assumed fibre CSA. Weibull statistics are used to model the strength of bast fibres.

New rules-of-mixture (ROM) have been reported which introduce additional parameters not normally required for synthetic fibre composites (porosity, fibre diameter distribution, FACF and yarn twist). In each case, these parameters default to unity when not applicable and the ROM reverts to the standard form. The evidence presented for each of the above models has only been validated for a small number of data sets. It would be appropriate for other researchers to confirm or refute the applicability of the recently proposed models. Successful development of these approaches should help to bring natural fibre composites to wider commercial application.

H   Acknowledgements

References

1. LH Koopmans, DB Owen and JI Rosenblatt, Confidence intervals for the coefficient of variation for the normal and log normal distributions, Biometrika, 1964, 51(1-2), 25-32.
2. I Harrop, J Summerscales, Acoustic emission testing of the structural integrity of multicore cable, British Journal of Non-Destructive Testing, July 1989, 31(7), 383-386.
3. MG Kendall and A Stuart, The Advanced Theory of Statistics 2, Charles Griffin and Co Ltd, London, 1961.
4. MT Huber, The theory of crosswise reinforced ferroconcrete slabs and its application to various important constructional problems involving rectangular slabs, Der Bauingenieur, 1923, 4(12), 354-360 and 4(13), 392-395.
5. J Summerscales, The bulk modulus of carbon fibres, Journal of Materials Science Letters, 2000, 19(1), 15-16.
6. E A Elsayed, Reliability Engineering, Addison Wesley Longman, 1996 ISBN 0201634813
7. Life Data Analysis Reference, ReliaSoft Publishing, 2005. Available on-line at: http://www.weibull.com/lifedatawebcontents.htm. (Accessed 22/08/08)
8. P Kittl and G Diáz, Weibull's fracture statistics, or probabilistic strength of materials: state of the art, Res Mech, 1998, 24(2). 99–207.
9. S van der Zwaag, The concept of filament strength and the Weibull modulus, Journal of Testing and Evaluation, September 1989, 17(5), 292–298.
10. SB Batdorf, Statistical fracture theories. In SM Lee (editor): International Encyclopedia of Composites - volume 6. VCH Publishers, New York, 1991, pp395–404 [ISBN 0-89573-736-1 (v6), ISBN 0-89573-290-4 (set)].
11. SL Phoenix and IJ Beyerlein, Statistical strength theory for fibrous composite materials. In A Kelly and C Zweben (editors): Comprehensive Composite Materials - volume 1 (T-W Chou – editor): Fibre reinforcements and general theory of composites, Elsevier, Oxford, 2000. pp 559–639 [chapter 1.19, ISBN 0-08-043719-2 (v1), ISBN 0-08-042993-9 (set)].
12. J Andersons, R Joffe, M Hojo, S Ochiai, Glass fibre strength distribution determined by common experimental methods, Composite Science and Technology, January 2002, 62 (1), 131-145.
13. K L Pickering and T L Murray, Weak link scaling analysis of high-strength carbon fibre, Composites Part A: Applied Science and Manufacturing, August 1999, 30 (8), 1017-1021.
14. L C Pardini, L G B Manhani, Influence of the testing gauge length on the strength, Young's modulus and Weibull modulus of carbon fibres and glass fibres, Materials Research, December 2002, 5(4), 411-420.
15. H W Herring, Selected mechanical and physical properties of boron filaments, TN D-3202, NASA, 1966.

16. A G Metcalf and G K Schmitz, Effect of length on the strength of glass fibres, Proceedings of the ASTM, 1964, 64, 1075-1093.
17. W J Padgett, S D Durham and A M Mason, Weibull analysis of the strength of carbon fibres using linear and power law models for the length effect, Journal of Composite Materials, September 1995, 29(14), 1873-1884.
18. J Andersons, E Spārniņš, R Joffe, L Wallstrom, Strength distribution of elementary flax fibres, Composite Science and Technology, March 2005, 65(3-4), 693-702.
19. K L Pickering, G W Beckerman, S N Alam and N J Foreman, Optimising industrial hemp fibre for composites, Composites Part A: Applied Science and Manufacturing, February 2007, 39(2), 461-468.
20. E Bodros and C Baley, Study of the tensile properties of stinging nettle fibres (Urtica dioica), Materials Letters, 2008, 62(14), 2143-2145.
21. Z P Xia, J Y Yu, L D Cheng, L F Liu and W M Wang, Study on the breaking strength of jute fibres using modified Weibull distribution, Composites Part A: Applied Science and Manufacturing, January 2009, 40(1), 54-59
22. N Defoirdt, S Biswas, L D Vriese, L Q N Tran, J V Acker, Q Ahsan, L Gorbatikh, A V Vuure, I Verpoest, Assessment of the tensile properties of coir, bamboo and jute fibres, Composites Part A: Applied Science and Manufacturing, May 2010, 41(5), 588-595.
23. N E Zafeiropoulos and C A Baillie, A study of the effect of surface treatments on the tensile strength of flax fibres: Part II. Application of Weibull statistics, Composites Part A: Applied Science and Manufacturing, February 2007, 38(2), 629-638.
24. L S Sutherland and C G Soares, Review of probabilistic models of the strength of composite materials, Reliability Engineering and System Safety, June 1997, 56(3), 183-196.
25. S B Batdorf and H L Heinisch, Weakest link theory reformulated for arbitrary fracture criterion, Journal of the American Ceramic Society, July 1978, 61 (7-8), 355-358.
26. AA Griffith, Phenomena of rupture and flow in solids, Philosophical Transactions of the Royal Society A, 1921, 221, 163–198.
27. G R Baran, J I McCool, K G Boberick and H Q Zhang, Size effect in resin/glass composite flexure strengths, Journal of Oral Rehabilitation, October 1999, 26, 775-780.
28. B Bohannan, Effect of size on bending strength of wood members, US Department of Agriculture - Forest Service - Forest Products Laboratory Research Paper FPL 56, Madison WI, May 1966.
29. J D Barrett, Effect of size on tension perpendicular to grain strength of Douglas-Fir, Wood and Fiber, 1974, 62 (2), 126-143.
30. A S Waltson and R L Smith, An examination of statistical theories for fibrous materials in the light of experimental data, Journal of Materials Science, 1985, 20 (9), 3260-3270.
31. M Lienkamp and P Schwartz, A Monte Carlo simulation of the failure of a seven fiber microcomposite, Composites Science and Technology, 1993, 46(2), 139–46.
32. WA Curtin, Tensile strength of fiber-reinforced composites: III. Beyond the traditional Weibull model for fiber strengths, Journal of Composite Materials, August 2000, 34(15), 1301–1332.
33. Yu Paramonov and J Andersons, A family of weakest link models for fibre strength distribution, Composites Part A: Applied Science and Manufacturing, April 2007, 38(4), 1227–1233.
34. IJ Myung, Tutorial on maximum likelihood estimation, Journal of Mathematical Psychology, February 2003, 47(1), 90-100.
35. Yong Cao, Yi-Qiang Wu and Koichi Goda, Development and application of composites reinforced with kenaf, Polymer Materials Science and Engineering, July 2008, 24(7), 11-15.
36. MJ John and S Thomas, Biofibres and biocomposites, Carbohydrate Polymers, 8 February 2008, 71(3), 343-364.
37. K Pickering, Properties and performance of natural-fibre composites, Woodhead Publishing, Cambridge, 2008. ISBN-13: 978 1 84569 267 4.
38. IM De Rosa, C Santulli and F Sarasin, Acoustic emission for monitoring the mechanical behaviour of natural fibre composites: a literature review, Composites Part A: Applied Science and Manufacturing, September 2009, 40(9), 1456-1469.
39. S Kalia, BS Kaith and I Kaur, Pretreatments of natural fibers and their application as reinforcing material in polymer composites - a review, Polymer Engineering and Science, 2009, 49(7), 1253-1272.
40. M Thiruchitrambalam, A Athijayamani, S Sathiyamurthy and A Syed Abu Thaheer, A review on the natural fiber-reinforced polymer composites for the development of Roselle fiber-reinforced polyester composite, Journal of Natural Fibers, 2010, 7(4), 307-323.
41. A Hassan, AA Salema, FN Ani and AA Bakar, A review on oil palm empty fruit bunch fiber reinforced polymer composite materials, Polymer Composites, 2010, 31(12), 2079-2101.

42. C Hill and M Hughes, Natural fibre reinforced composites opportunities and challenges, Journal of Biobased Materials and Bioenergy, June 2010, 4(2), 148-158.

43. JK Pandey, SH Ahn, CS Lee, AK Mohanty and M Misra, Recent advances in the application of natural fiber-reinforced composites, Macromolecular Materials and Engineering, 2010, 295, 975–989.

44. J Summerscales, N Dissanayake, W Hall and AS Virk, A review of bast fibres and their composites. Part 1: fibres as reinforcements, Composites Part A: Applied Science and Manufacturing, October 2010, 41(10), 1329-1335.

45. J Summerscales, N Dissanayake, W Hall and AS Virk, A review of bast fibres and their composites. Part 2: composites, Composites Part A: Applied Science and Manufacturing, October 2010, 41(10), 1336-1344.

46. H Ku, H Wang, N Pattarachaiyakoop and M Trada, A review on the tensile properties of natural fiber reinforced polymer composites, Composites Part B: Engineering, June 2011, 42(4), 856-873.

47. FP La Mantia and M Morreale, Green composites: a brief review, Composites Part A: Applied Science and Manufacturing, June 2011, 42(6), 579-588.

48. E Zini and M Scandola, Green composites: an overview, Polymer Composites, 2011, 32(12), 1905-1915.

49. T Mukherjee and N Kao, PLA based biopolymer reinforced with natural fibre: a review, Journal of Polymers and the Environment, September 2011, 19(3), 714-725.

50. M Hughes, Defects in natural fibres: their origin, characteristics and implications for natural fibre-reinforced composites, Journal of Materials Science, 2012, 47(2), 599-609.

51. MM Kabir, H Wang, KT Lau and F Cardona, Chemical treatments on plant-based natural fibre reinforced polymer composites: an overview, Composites Part B: Engineering, October 2012, 43(7), 2883-2892.

52. DB Dittenber and HVS GangaRao, Critical review of recent publications on use of natural composites in infrastructure, Composites Part A: Applied Science and Manufacturing, August 2012, 43(8), 1419-1429.

53. AS Virk, W Hall and J Summerscales, Physical characterisation of jute technical fibres: fibre dimensions, Journal of Natural Fibres, 2010, 7(3), 216-228.

54. AS Virk, W Hall and J Summerscales, Modulus and Strength Prediction for Natural Fibre Composites, Materials Science and Technology, July 2012, 28(7), 864-871.

55. M Aslan, G Chinga-Carrasco, BF Sørensen and B Madsen, Strength variability of single flax fibres, Journal of Materials Science, 2011, 46(19), 6344-6354.

56. JL Thomason, J Carruthers, J Kelly and G Johnson, Fibre cross section determination and variability in sisal and flax and its effect on fibre performance characterisation, Composites Science and Technology, 4 May 2011, 71(7), 1008-1015.

57. B Cosson, S Comas-Cardona, S Bickerton, JM Gan, F Zhang and C Binetruy, An optically based inverse problem to measure in-plane permeability fields, The 10th International Conference on Flow Processes in Composite Materials (FPCM10), Monte Verità - Ascona (Switzerland), 11-15 July 2010.

58. AS Virk, Numerical models for natural fibre composites with stochastic properties, PhD thesis, University of Plymouth, 2010, http://pearl.plymouth.ac.uk/handle/10026.1/303.

59. E Bradbury (University of Plymouth), private communication, 02 April 2012.

60. AS Virk, W Hall and J Summerscales, Strain as the key design criterion for failure of natural fibre composites, Composites Science and Technology, June 2010, 70(6), 995-999.

61. AS Virk, W Hall and J Summerscales, The tensile properties of jute fibres, Materials Science and Technology, October 2009, 25(10), 1289-1295.

62. AS Virk, W Hall and J Summerscales, Multiple data set (MDS) weak-link scaling analysis of jute fibres, Composites Part A: Applied Science and Manufacturing, November 2009, 40(11), 1764-1771.

63. AS Virk, W Hall and J Summerscales, Modelling tensile properties of jute fibres, Materials Science and Technology, January 2011, 27(1), 458-460.

64. J Andersons, E Poriķe and E Spārniņš, Ultimate strain and deformability of elementary flax fibres, Journal of Strain Analysis, August 2011, 46(6), 428-435.

65. T Hänninen, A Thygesen, S Mehmood, B Madsen and M Hughes, Mechanical processing of bast fibres: the occurrence of damage and its effect on fibre structure, Industrial Crops and Products, 2012, 39, 7-11.

66. D Dai and M Fan, Characteristic and performance of elementary hemp fibre, Materials Scoiences and Applications, 2010, 1(6), 336-342.

67. A Thygesen, B Madsen, AB Bjerre and H Lilholt, Cellulosic fibers: effect of processing on fiber bundle strength, Journal of Natural Fibers, 2011, 8(3), 161-175.

68. J Andersens, E Spārniņš, E Porike and R Joffe, Strtength distribution of elementary flax fibres due to mechanical defects, 11th International Inorganic-Bonded Fiber Composites Conference, Madrid, 5-7 November 2008, 247-253.

69. FJ Guild and J Summerscales, Microstructural image analysis applied to fibre composite materials: a review, Composites, 1993, 24(5), 383-394.

70. J Summerscales, Microstructural characterisation of fibre-reinforced composites, Woodhead Publishing, Cambridge, 1998. ISBN 978-1-85573-756-3.

71. J Summerscales, NRL Pearce, P Russell and FJ Guild, Voronoi cells, fractal dimensions and fibre composites, Journal of Microscopy, February 2001, 201(2), 153-162.

72. JK Mackenzie, The elastic constants of a solid containing spherical holes, Proceedings of the Physical Society, 1950, B63(2), 2-11.

73. JB Wachtman, Elastic deformation of ceramics and other refractory materials, In JB Wachtman (editor): NBS Special Publication 303 - Mechanical and Thermal Properties of Ceramics, , National Bureau of Standards, Washington DC, 1969, pages 139-168.

74. RW Davidge, Mechanical Behaviour of Ceramics, Cambridge University Press, Cambridge, 1979. ISBN 0-521-29309-x.

75. B Madsen and H Lilholt, Physical and mechanical properties of unidirectional plant fibre composites—an evaluation of the influence of porosity, Composites Science and Technology, 2003, 63(9), 1265–1272

76. H Toftegaard and H Lilholt, Effective stiffness and strength of flax fibres derived from short fibre laminates, Proceedings of the 23rd Risø International Symposium on Materials Science: Sustainable Natural and Polymeric Composites - Science and Technology, Roskilde, 2-5 September 2002, 325-334. ISBN 87-550-3091-2.

77. B Madsen, A Thygesen and H Lilholt, Plant fibre composites – porosity and stiffness, Composites Science and Technology, 2009, 69(7-8), 1057-1069.

78. H Krenchel, Fibre Reinforcement, Akademisk Forlag, Copenhagen, 1964 (DSc thesis, Technical University of Denmark, 1963).

79. B Lamy and C Baley, Stiffness prediction of flax fibers-epoxy composite materials, Journal of Materials Science Letters, 1 June 2000, 19(11), 979-980.

80. J Summerscales, W Hall and AS Virk, A fibre diameter distribution factor (FDDF) for natural fibre composites, Journal of Materials Science, 2011, 46(17), 5876-5880.

81. PJ Roe and MP Ansell, Jute-reinforced polyester composites, Journal of Materials Science, 1985, 20 (11), 4015-4020.

82. P Kumar, Mechanical Behaviour of Jute Fibres and their Composites, Indian Journal of Technology, 1986, 24 (1), 29-32.

83. J Gassan and A K Bledzki, Possibilities for improving the mechanical properties of jute/epoxy composites by alkali treatment of fibres, Composite Science and Technology, July 1999, 59 (9), 1303-1309.

84. RA Clark and MP Ansell, Jute and glass fibre hybrid laminates, Journal of Materials Science, 1986, 21(1), 269-276.

85. KS Ahmed, S Vijayarangan and ACB Naidu, Elastic properties, notched strength and fracture criterion in untreated woven jute-glass fabric reinforced polyester hybrid composites, Materials and Design, 2007, 28 (8), 2287-2294.

86. AN Shah and SC Lakkad, Mechanical properties of jute-reinforced plastics, Fibre Science and Technology, July 1981, 15 (1), 41-46.

87. TM Gowda, ACB Naidu and R Chhaya, Some mechanical properties of untreated jute fabric-reinforced polyester composites, Composites Part A: Applied Science and Manufacturing, 1999, 30 (3), 277-284.

88. Y Rao and RJ Farris, A modeling and experimental study of the influence of twist on the mechanical properties of high-performance fiber yarns, Journal of Applied Polymer Science, 29 August 2000, 77(9), 1938–1949.

89. NK Naik and Y Madhavan, Twisted impregnated yarns: elastic properties, Journal of Strain Analysis for Engineering Design, 1 January 2000, 35(2), 83-91.

90. J Baets, D Plastria, J Ivens and I Verpoest, Determination of the optimal flax fibre preparation for use in UD flax-epoxy composites, Proc. 4th International Conference on Sustainable Materials, Polymers and Composites, Birmingham, 6-7 July 2011.

91. J Baets, D Plastria, J Ivens and I Verpoest, Determination of the optimal flax fibre preparation for use in UD-epoxy composites, Proc. ICCM-18: 18th International Conference on Composite Materials, Jeju - Korea, 21-26 August 2011.

92.   B Madsen, P Hoffmeyer, AB Thomsen and H Lilholt, Hemp yarn reinforced composites. I: yarn characteristics, Composites Part A: Applied Science and Manufacturing, 2007, 38(10), 2194-2203.
93.   DU Shah, PJ Schubel and MJ Clifford, Modelling the effect of yarn twist on the tensile strength of unidirectional plant fibre yarn composites, Journal of Composite Materials, published online 13 March 2012.
94.   EC McLaughlin and RA Tait, Fracture mechanism of plant fibres, Journal of Materials Science, 1980, 15(1), 89-95.
95.   S Goutianos and T Peijs, The optimisation of flax fibre yarns for the development of high-performance natural fibre composites, Advanced Composites Letters, 2003, 12(6), 237-241.
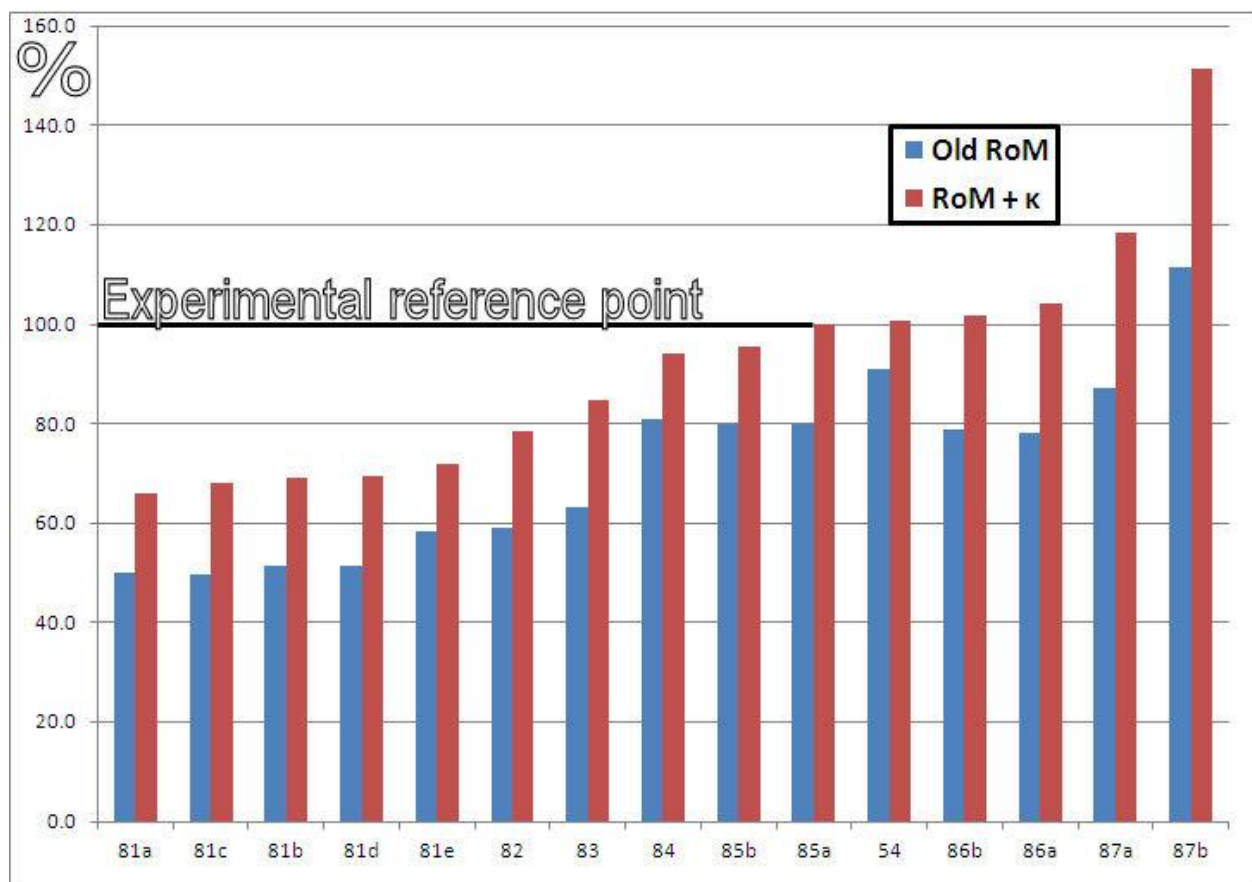
Figure 1: Comparison of predicted moduli from rule of mixtures without (blue) and with (red) the Fibre Area Correction Factor. The x-axis numbers are the respective references from which the data was extracted for analysis with the letters indicating individual data sets (reference 54 is data from the authors of this paper).